Real-Time Embedded EMG Signal Analysis for Wrist-Hand Pose Identification

Real-Time Embedded EMG Signal Analysis for Wrist-Hand Pose Identification

Sumit A. Raurale, *Student Member, IEEE,* John McAllister, *Senior Member, IEEE* and Jesus Martinez del Rincon, *Member, IEEE*

***Abstract*—Electromyographic (EMG) signals sensed on the forearm skin surface, when placed over specific muscles, enable a wide range of wrist-hand movements to be accurately detected via complex time-frequency EMG analysis. This capability, however is not available for EMG wearables, which sense EMG from random positions and experience substantially reduced detection performance as a result. In addition, the complexity of the time-frequency analysis process currently precludes real-time detection using the simple embedded processors on EMG wearables is not possible. This paper describes an approach which resolves both these shortcomings. It shows that, when random sensor placement is adopted, wrist-hand movement detection with performance equal the state-of-the-art can be achieved, with only 10% of the computational complexity. This latter property allows the first real-time wrist-hand movement detector using only simple embedded processors; specifically when using on ARM Cortex-A53 processor, execution time is lowered by 90% against the state-of-the-art, with no reduction in detection performance. It is shown how this can be further reduced by 30% by using fewer EMG channels or features, whilst maintaining good detection performance. To the best of the authors' knowledge, this is the first record of real-time high-performance wrist-hand movement detection for standalone, battery-powered EMG wearables.**

***Index Terms*—Electromyographic (EMG), commodity EMG sensors, time-domain features, linear discriminant analysis (LDA), multilayer perceptron (MLP), operational complexity.**

I. Introduction

BIOPHYSICAL signals, such as Electroencephalogram (EEG), Electrocardiogram (ECG) or neural signalling [1], [2] are increasingly used to biometric identification, monitoring physical well-being or controlling electronic devices. Electromyographic (EMG) signals fall into this class of phenomena and their interpretation has found a number of practical uses in human-computer interface applications, such as immersive environments, video games, electronic gadgets or control of robotic devices or 'bionic' limbs [3]. These applications have given rise to wearables [4]–[7] which use skin's surface sensors to measure EMG signals.

Numerous approaches have shown that a wide range of wrist-hand movements can be detected with high accuracy by analysis of lower-arm EMG signals [3], [8]–[10]. These approaches, however, all make the same assumption: EMG sensors are placed precisely over specific arm muscles. They all rely on complex frequency-domain analysis of the EMG signals they measure, which cannot be realised in real-time using the simple embedded processors housed in EMG wearables. High performance, real-time detection of wrist-hand movements from EMG requires precision placement of sensors and substantial processing resource.

Wearables violate the first assumption. They do not place sensors over specific muscles, rather acquiring EMG from sensors whose location is random and changes every time the wearable is removed and refitted. Their detection performance is significantly lower than the state-of-the-art [4]–[7]. The authors are not aware of any work which uses this sensing modality yet maintains state-of-the-art detection performance.

This experimental work extends [11] to make the following contributions:

1) It is shown how the class-leading EMG wrist-hand detection approach [8] is ineffective when EMG sensors are randomly-placed, enabling only 73% accurate detection for nine wrist-hand movements.
2) It is shown that time-domain analysis of EMG signals from randomly-placed sensors enables detection accuracy of 99% - beyond the state-of-the-art - with less than 10% of the computational complexity.
3) It is shown that the aforementioned complexity reductions enables the first real-time EMG wrist-hand movement detector using an ARM Cortex A-53 embedded processor suitable for integration in EMG wearables.
4) It is shown how the complexity of the proposed approach can be further reduced by over 30% whilst maintaining the breadth and accuracy of the current state-of-the-art.

The structure of this paper is as follows. Section II presents the state-of-the-art in EMG acquisition and analysis for identification of wrist-hand poses, before Section 3 introduces our proposed approach and quantifies its classification accuracy. Sections 4 and 5 then, respectively, analyse the complexity of the proposed approach and its embedded deployment, and explore performance-cost trade-offs.

II. Previous Work

A. Wrist-Hand Movement Detection using EMG

When acquiring skin-surface EMG, there are two possible approaches: either the EMG sensors are placed over specific arm muscles (known henceforth as the placed-sensor approach), or they can be randomly-placed. The placed-sensor approach is the much more comprehensively investigated. The precise placement over specific muscles is important, because

Manuscript received April 19, 2018; revised August 26, 2018.

This work is funded by the Engineering and Physical Sciences Research Council (EPSRC), UK.

The authors are with the Institute of Electronics, Communications and Information Technology (ECIT), Queen's University of Belfast, UK. (e-mail: sraurale01@qub.ac.uk; jp.mcallister@ieee.org; j.martinez-del-rincon@qub.ac.uk)

it minimises the level of interference and crosstalk in the acquired signal as a result of movement in nearby muscles [12], [13]. The sensors are placed between a motor point and either another such point, or a tendon insertion [12]. This approach allows a wide range of movements to be detected accurately [14] via a spectrum of different techniques.

In placed-sensor approaches, the acquired EMG signals undergo time-frequency analysis, enabled by the differing frequency characteristics of the EMGs emanating from the muscles over which they are placed. These techniques include Fourier transform [15], Wavelet Transform (WT), and Wavelet Packet Transform (WPT) [8], [9], [14], [16]. For instance, the work in [16] derives a feature vector, using Discrete Wavelet Transform (DWT), which is then projected via unsupervised Principal Component Analysis (PCA) [17] to detect six different hand poses with 97.50% accuracy. Numerous other recent studies have used PCA for feature projection in various applications [8], [16], [18]. The work in [8] combines PCA with a Self-Organizing Feature Map (SOFM) to enable a combined linear/non-linear unsupervised feature projection method. If linear supervised projection is required Linear Discriminant Analysis (LDA) is preferred due to its class separability [9], [19], [20] and its superior performance as compared to PCA/SOFM [20]. The final step in the EMG processing sequence is inference of movements from the reduced-dimensionality feature vectors. Various classifiers have been analysed in this context, including Support Vector Machines (SVMs) [9], [10], [18], [21], [22], bayesian classifiers [14], gaussian mixture models [14], hidden markov models [14], fuzzy classifiers [14] and Multilayer Perceptrons (MLPs) [8], [16], [20], [23].

A large body of work has addressed the specific problem of EMG-based inference of wrist-hand movements. In [24], three hand motions are differentiated using 1D Local Binary Pattern (LBP) feature extraction. Four sensors are used in [15] to detect seven wrist-hand movements using time and frequency domain features with SVM classification, whilst [22] also uses four sensors on the lower and upper forearm to classify six wrist-hand motions with accuracy between 87 - 97%. In [25], hand-finger movements were classified with 94.30% accuracy using bicoherence analysis and extreme learning machine techniques. Finally, [26] describes a system using eight placed sensors, DWT characterisation and an artificial neural network classifier to achieve 91.86% classification accuracy. Amongst this body of work, however, the approach in [8] stands out in both the breadth and accuracy of its capabilities. By employing Local Discriminant Basis (LDB) with WPT, PCA-based projection and MLP-based classification, nine wrist-hand movements can be detected with 97.40% accuracy.

B. Motivation

The works discussed above show that high-performance wrist-hand movement detection - classifying a wide range of movements with high accuracy - from EMG is certainly possible. However, these works all assume sensors placed precisely over specific arm muscles. The authors are unaware of any approach which maintains this performance without precise placement of sensors.

For an emerging class of wearable EMG acquisition devices, the placed-sensor assumption is invalid. These rely on sensors which are both randomly positioned and whose position can change every time the devices is removed and refitted. For instance, the unit used in [4]–[7] composes an armband of eight EMG sensors. Detection performance using this sensing modality leads to significantly reduced - [4]–[7] report a maximum of five movements detected. Relatedly, a second major characteristic of high-performance detection systems is complexity: the frequency domain algorithms used preclude real-time detection using the types of embedded processor which can be embedded in EMG wearables. The authors are unaware of any real-time high-performance wrist-hand movement detection schemes which do not require substantial remote computing resource.

This paper address these shortcomings. It challenges the assumption that placed sensors are required to achieve high detection performance. Its objectives are to enable:

- High performance wrist-hand movement detection, in terms of both the breadth and accuracy of movement detection, using randomly-placed multi-channel EMG sensors.
- Real-time detection using an embedded processor suitable for integration in a portable, battery-powered device.

III. Movement Acquisition and Classification

The state-of-the-art in wrist-hand movement inference from placed-sensor EMG acquisition systems differentiates nine different movements:

(i) hand open
(ii) wrist flexion
(iii) wrist pronation
(iv) wrist ulnar flexion
(v) relaxation
(vi) wrist supination
(vii) hand close
(viii) wrist extension
(ix) wrist radial flexion

This work aims to detect the same set of movements with similar accuracy to placed-sensor approaches. The 200 Hz per channel [27] sampling frequency is sufficient for this work because whilst in general the frequency range of EMG signals is between 0-1000 Hz, the dominant energy is concentrated in the range of 20-500 Hz [8], [20], and further restricting to 200 Hz does not necessarily degrade system performance [28]. Current wrist-hand inference processes use 256-sample windows of EMG data per sensor, with 128ms offset between successive windows [8], [20]. We use the same, making 128 per window the upper limit for real-time detection. [29].

A. EMG Features

As described in Section II, placed-sensors acquisition approaches measure EMG signals from the skin's surface directly over specific arm muscles; the unique frequency composition of each muscle's EMG then enables effective frequency-domain analysis. If randomly-placed, however, the EMG at

each sensor is a mixture of those produced by many muscles, and frequency-domain specialisation is ineffective. Hence time-domain analysis is used in this case.

Twenty-six time-domain features were proposed for this problem by Phinyomark *et al* [30]. Based on the minimum redundancy feature selection, we propose to use only eight features set to characterise the signal emanating from each EMG sensor.

- **Integrated EMG** (IEMG): EMG measures change in potential levels between muscle contraction and the stationary state. IEMG detects the muscle activation condition as an onset index by illustrating the firing point within activation of muscle contraction levels.

$$IEMG = \sum_{n=1}^{N} \mid x_n \mid \tag{1}$$

- **Mean Squared Value** (MSV): also detects muscle activation condition as an onset index.

$$MSV = \frac{1}{N} \sum_{n=1}^{N} {x_n}^2 \tag{2}$$

- **Variance**: estimates power density.

$$VAR = \frac{1}{N-1} \sum_{n=1}^{N} \mid x_n - \mu \mid^2 \tag{3}$$

where μ is the mean value of x.

- **Root Mean Square** (RMS): represents fatigue in the muscle contraction levels whilst changing movement within each window [31], [32]. It is expressed as:

$$RMS = \sqrt{\frac{1}{N} \sum_{n=1}^{N} x_n^2} \tag{4}$$

- ln **RMS**: characterises the differences in RMS magnitude, amplifying relatively small absolute RMS values
- **Kurtosis**: characterises the sharpness of the EMG sample distribution [33]. Describes the change in muscle activation levels whilst contracting and is higher during strong contractions of different movements, providing high variation for different classes of movement. It also measures differentiates between less/more outlier-prone distributions using a threshold value of 3:

$$k = \left\{ \frac{1}{N} \sum_{n=1}^{N} \left[\frac{x_n - \mu}{\sigma} \right]^4 \right\} - 3 \tag{5}$$

where σ is the distribution's standard deviation of x.

- **Skewness**: measures the asymmetry of different muscle contraction distributions [34].

$$s = \frac{1}{N} \sum_{n=1}^{N} \left[\frac{x_n - \mu}{\sigma} \right]^3 \tag{6}$$

- **Auto-regressive Model** (ARM): predicts intramuscular EMG and its spectral properties [35] [36]. Describes each sample of the EMG signal as a linear combination of the previous samples plus a white noise error term $w[n]$ [15], [30], [31], [37]

$$A_n = \sum_{p=1}^{P} a_{p,n} x_{n-p} + w_n \tag{7}$$

where a_p are the AR coefficients, w_n white noise and P is the order of the AR model (6 in our case, evaluated using the Akaike information criterion [38]). A constraint model is obtained using the stochastically perturbed difference equation constraint model [39],

$$\bigtriangledown a_{p,n} = \delta_{p,n} \tag{8}$$

where $p = 1 \cdots P$ and δ_p is assumed to be a zero-mean Gaussian white noise sequence with variance $\tau_p^2 = \tau^2$.

These features were selected from twenty-six based on their correlation statistics. Correlation coefficients for all features [30] were evaluated, resulting in a mean $r_\mu = 0.8$. Any features with larger correlation coefficients are not used. The correlation coefficients for the proposed features is summarised in Fig. 1.

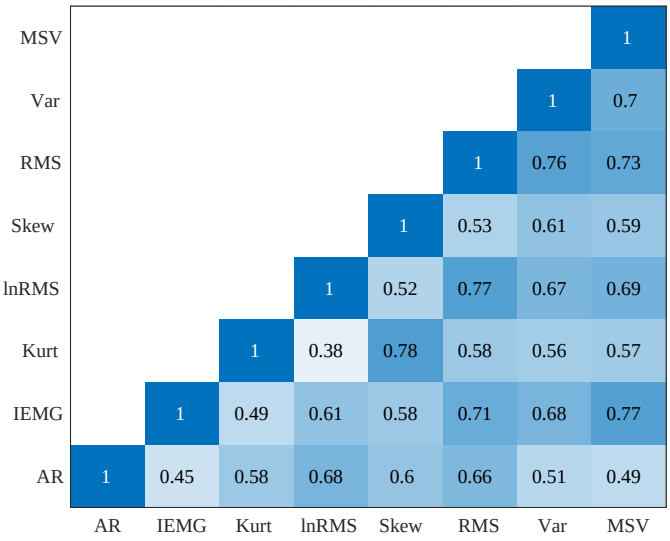

Fig. 1: Correlation coefficients for different time domain features.

The remaining eight time-domain capable of extracting the fundamental information from EMG signal *viz.* muscle contraction, activity detection, onset detection, and power density. To tell different movements apart most accurately, features should provide as wide a range of values as possible. The variation in the normalised amplitude for each of the eight features across the nine wrist-hand movements is summarised in Fig. 2 (normalisation factors are quoted in circular braces). The eight features are ordered in decreasing order of variation.

When represented by their l_2 norm, the vectors of AR coefficients shows the highest range of amplitude - 5.80 to 60.10 across the nine movements; this is followed by IEMG (7.53 - 34.04), kurtosis (2.17 - 8.23) and lnRMS (1.93 to 5.89). The remaining features - skewness, RMS, variance and MSV have, relatively speaking, lower variation but can still contribute to increasing performance.

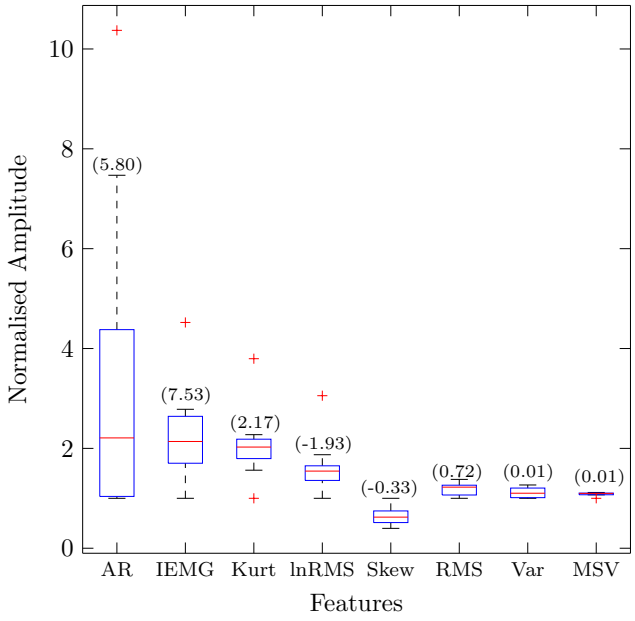

Fig. 2: Amplitude variation of different time domain features for nine wrist-hand movements.

These features are calculated for each 256 sample window from each of the eight EMG channels acquired by the armband. That is, the eight-channel EMG signal measured by the EMG armband is segmented into 256 time-sample windows $\mathbf{X}_N \in \mathbb{R}^{256\times 8}$. From each channel is derived a feature vector $\mathbf{f}_c \in \mathbb{R}^{13}$ composed of the features (including a six-element AR coefficient vector) described above.

B. Feature Projection & Classification

The purpose of feature projection is to reduce the dimensionality of the incoming time-domain feature vectors by projecting the data points onto a lower-dimensional feature space. Then, classification infers the hand-wrist pose represented by each vector by classifying it into one of nine classes, each corresponding to one of the known wrist-hand poses.

The 13-element feature vectors emanating from each of the eight EMG channels are concatenated into a single vector $\mathbf{f} \in \mathbb{R}^{104}$. Feature projection creates an appropriate subset of new features from an original feature set such that the learning criterion is optimized [19]. For EMG signal analysis, PCA and LDA have been popularly used for this purpose [9], [19], [20]. The most effective choice will be that which, when combined with the proposed classifier, enables the highest classification accuracy. Similarly, a set of alternative classifiers may also be considered, including SVM [9], [22], k-Nearest Neighbour (k-NN) and MLP [8], [14], [30]. The work in [8], [20] has shown that employing MLP to classify time-frequency feature vectors is able to differentiate the nine classes of wrist-hand movements desired in the proposed approach, and as such a similar approach is considered here.

C. System Evaluation

The relative performance of SVM, k-NN and MLP classifiers, along with LDA or PCA feature projection are empirically compared to determine the best combination. The proposed system architecture is illustrated in Fig. 3.

Both the LDA and PCA feature projection options project each $\mathbf{f} \in \mathbb{R}^{104}$ input feature vector onto a compressed equivalent $\mathbf{f}' \in \mathbb{R}^{8}$. The dimensionality of the resulting vector is chosen to be one less than the number of classes into which the vectors are to be classified - i.e. the number of hand-wrist poses [40]. The MLP classifier option is configured with three hidden layers comprised of a total of forty-four neurons and a nine-neuron output layer, with a single output neuron for each of the nine hand motions to be recognized[1].

In order to compare the breadth and accuracy of the proposed time-domain approach to the state-of-the-art in placed-sensor systems, it is benchmarked against the approach in [8], [20], which can differentiate nine movements with accuracy exceeding 97% on average. To ensure fair comparison, we adopted the same testing approach quoted in [8], [20]. Ten subjects (seven male, three female) aged 27 $\pm$ 4 years each provided ten training samples for each of nine movements, and testing was performed on a further ten instances of each movement. Each subject was instructed to be seated on a height adjustable chair in a comfortable position with their elbow and forearm initially resting on a horizontal surface. The subject was then instructed to raise their hand perpendicular to surface before performing the target wrist-hand movements. Each movement was conducted for approximately 1 second from the rest position and maintained in the target position for 5 seconds. The movements were performed in a fixed order for each subject. For testing, different movements were considered in a random order. During training, the MLP weights and bias are initially drawn from a uniform distribution with a mean and variance of 0 and 1, respectively. The learning process was stopped when the absolute rate of change in the average squared error per iteration was sufficiently small [41].

D. Training

Training follows the same strategy as that employed in the leading placed-sensor approach with which we compare [20]. In the training data set, each sample consists of total 72 windows (with each window tagged with the corresponding movement) - eight windows for each of nine movements for each session of ten people. From each 256-sample window is the derived a feature vector $\mathbf{f} \in \mathbb{R}^{H}$ where H is number of feature coefficients (104 as evaluated in Section III-A). Thus, 10 sessions from each of 10 subjects produces 800 feature vectors for each movement. In total the training data frame is thus $D \in \mathbb{R}^{J\times H}$, where $J = 7200$ is the total number of feature vectors from all nine movements. In addition a class label vector defines each feature data class in D to train the LDA and derive the following parameters:

1) Mean feature-vector $\bar{\mathbf{f}} \in \mathbb{R}^{H}$ of D;

[1]This configuration was determined by empirical observation of the error rate as the number of neurons was varied.

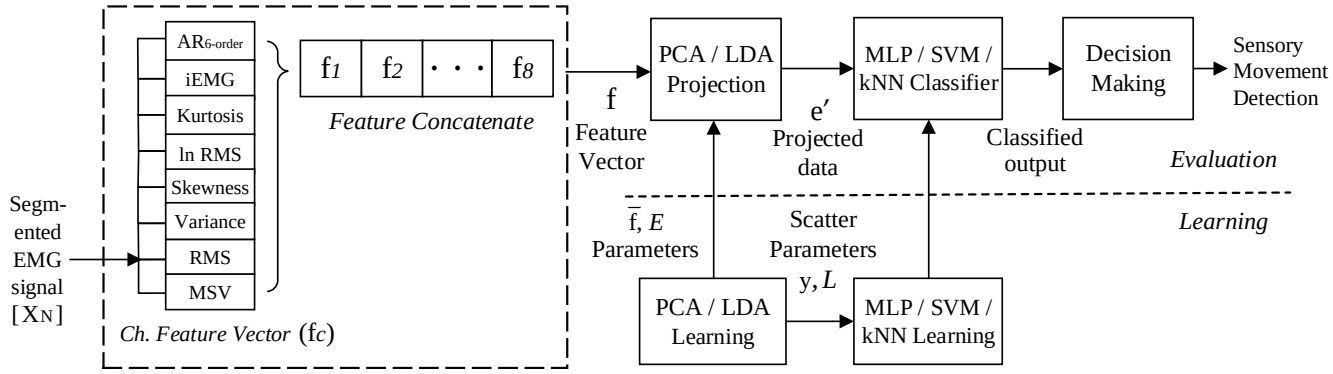

Fig. 3: Proposed System Architecture

2) Matrix of eigenvectors $E \in \mathbb{R}^{p \times H}$ where $p = 8$ sorted eigenvalues of D;
3) Matrix of scatter feature projection $L \in \mathbb{R}^{J \times p}$ of the training data matrix D;
4) Vector of class labels $\mathbf{c}' \in \mathbb{R}^{J}$ representing the training data matrix D;
5) Vector $\mathbf{e} \in \mathbb{R}^{p}$ of sorted eigenvalues of D;

In the case where PCA is used, as well as deriving L as in LDA, a matrix $P \in \mathbb{R}^{J \times p}$ of the principal component vectors of D is derived and used to train the classifiers.

In the case where MLP is used to realise the classifier, the training phase derives from L (LDA) or P (PCA) the weights for each neuron connection in the graph. In the case where SVM is used as the classifier, the training phase derives from L (LDA) or P (PCA) a variable-sized set of support vectors for the points on the boundaries between classes.

Ten-fold cross-validation was performed on the training data using the proposed features, LDA and MLP. The optimal MLP configuration was selected based on maximum classification accuracy. The system is tested on the remaining dataset.

E. Testing

The performance of the system is tested on ten sessions of data from the same 10 subjects, to again ensure consistent comparison with [20]. An EMG window is extracted from each of the $c = 8$ channels $\mathbf{X}_c \in \mathbb{R}^{256}$ and the features in Section III-A derived. The resulting feature vectors $\mathbf{f}_c \in \mathbb{R}^{13}$ are concatenated into $\mathbf{f} \in \mathbb{R}^{108}$ used to derive $\mathbf{e}' \in \mathbb{R}^{p}$:

$$\mathbf{e}' = (\mathbf{f} - \bar{\mathbf{f}}) \times E^{T} \tag{9}$$

The output vector $\hat{\mathbf{y}} \in \mathbb{R}^{9}$ is evaluated from the trained model parameters from $\mathbf{e}'$.

The performance of MLP, SVM and k-NN classifiers ($k = 3$) with either LDA or PCA feature projection are compared. The relative performances of these configurations across all nine wrist-hand movements is described in Fig. 4.

The results in Fig. 4 are rather definitive. They suggest that combining LDA feature projection and MLP-based classification enables a clear benefit in the accuracy with which the time-domain features are classified. Specifically, the accuracy of this combination exceeds 98% for each individual

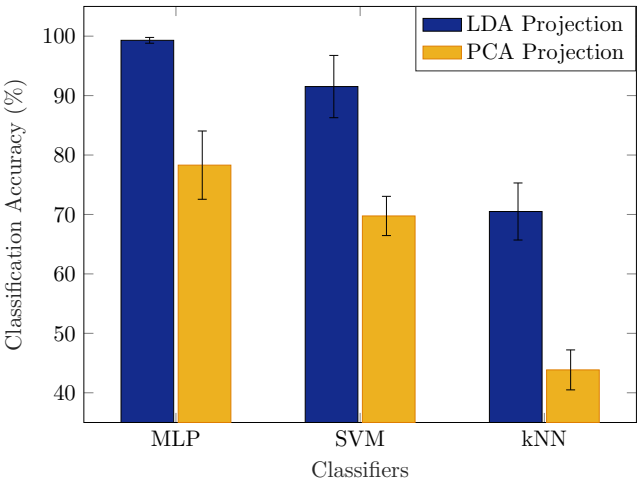

Fig. 4: Classification results of different feature classifiers.

movement, and 99% on average. This accuracy substantially exceeds any other approach, with a combination of LDA and SVM achieving in excess of 91% accuracy overall, whilst no other approach exceeds 80% accuracy and performance reduces to below 50% using PCA/kNN.

It is noticeable that, for a similar range of movements, this level of accuracy is comparable with and, indeed, beyond that of time-frequency approaches for placed-sensor acquisition [8], [14], [16], [20], [26], [42], as surveyed in Section II. To recap, the state-of-the-art approach surveyed achieved an average of 97.4% accuracy when classifying nine wrist-hand movements. This is less marginally less than the 99% observed in the proposed approach, for the same range of movements. In addition, this accuracy is observed when placed-sensor acquisition is used. If the same approach adopted in [8], [20] were applied to the randomly-placed sensing regime, then the performance observed is as summarised in Table I.

As this shows, when the sensor used to capture EMG signals are not placed over specific muscles, the performance of time-frequency analysis is severely diminished. Specifically, when the state-of-the-art WPT-based time-frequency approach in [20] is applied to EMG data from randomly-placed sensors, classification accuracy is approximately 72% or 48%, depend-

TABLE I: Comparison of Time and Time-Frequency Classification Schemes

Movement	Classification Accuracy (%)			
	Time-domain		Time-frequency	
	LDA	PCA	LDA [20]	PCA [8]
Hand open	99.90	90.60	76.00	48.35
Hand close	99.75	68.40	80.50	51.30
Wrist flexion	99.65	78.50	77.30	47.35
Wrist extension	98.95	73.30	70.50	41.90
Wrist pronation	99.80	82.70	61.90	45.65
Wrist supination	95.55	77.50	72.40	50.45
Wrist ulnar flexion	98.60	76.80	64.70	48.65
Wrist radial flexion	99.15	78.10	75.10	48.10
Relaxation	99.40	78.90	76.80	49.85
Total	**99.30**	**78.30**	**72.80**	**47.95**

ing on the feature projection technique employed.

To the best of the authors' knowledge, this is the first record of a randomly-placed EMG sensing modality enabling wrist-hand movement detection with performance comparable to the state-of-the-art. All other approaches of similar performance use precision-placed sensors. Indeed, the accuracy of the results in Table I are beyond the state-of-the-art. It is also worth noting that the number of movements which can now be accurately detected, given the sensing modality, has almost doubled from 5 [4]–[7] to 9.

Classification performance is only one metric when considering the design of practical EMG acquisition and classification systems. Many others - such as throughput, latency, energy expenditure - influence other aspects of the system's behaviour, such as its battery life or level of heat dissipation. These are heavily influenced by the complexity of the proposed classification scheme and can limit the ability to realise real-time EMG analysis such as that proposed on practical, portable, battery-operated devices. The complexity of the proposed approach and its performance is considered in Section IV.

IV. Complexity

To determine the complexity of the proposed time-domain wrist-hand inference system, the analytical approach described in [43] is adopted. It is assumed that each primitive arithmetic, logical or comparison operator accounts for one operation, as do conditional operations. Under these assumptions, the complexity of deriving each time-domain feature is quoted alongside the LDA feature projection operation and the MLP classifier in Table II. Note that these are expressed in terms of a number of key operating parameters of the system, the names and meaning of which are quoted in Table III, along with the values of each taken in the system described in Section III.

As Table II describes, the worst-case complexity of the proposed approach can be expressed as $O(u[PN+qk]+qlr)$ where u is the number of EMG channels, P the order of AR model and N the width of the EMG segment. This can

TABLE II: Time-Domain EMG Classification Complexity

Technique	Complexity
AR	$u[P(2N+21)]$
IEMG	$u(2N+4)$
Kurtosis	$u(4N+2)$
log RMS	$u(N+1)$
Skewness	$u(3N+2)$
RMS	$u(2N+6)$
Variance	$u(3N+4)$
MSV	$u(2N+5)$
Features	$u[P(2N+21)+17N+24]$
LDA	$[q-1]\,(2uk+3)$
MLP	$[q-1]\,[l(3r+6)]$
Total	$u[P(2N+21)+17N+24]+$ $[q-1][(2uk+3)+l(3r+6)]$

TABLE III: System Complexity Parameters

Parameter	Represents	Value Taken
u	Number of channels	8
N	Width of segmented window	256
P	Order of AR model	6
q	Number of movements	9
k	Width of time-domain feature vector	13
r	Number of neurons in MLP	61
l	Number of hidden layers in MLP	3

TABLE IV: Time-Frequency Classification Complexity

Technique	Complexity
WPT	$u[2D(18N\times log(3N)+18)]$
LDA	$[q-1]\,(2g+3)$
MLP	$[q-1]\,[l(3r+6)]$
Total	$u[2D(18N\times log(3N)+18)]+$ $[q-1][(2g+3)+l(3r+6)]$

be compared to the complexity of the state-of-the-art placed-sensor classification approach used to benchmark performance in Section III-C [8], [20]. Table IV describes the parameterised complexity of this approach and Table V the relevant parameters.

TABLE V: Time-Frequency System Parameters

Parameter	Represents	Value Taken
D	Number of decomposition layers in WPT	3
g	Width of WPT feature vector	2048

For this time-frequency approach, WPT feature vector derivation has complexity $O(u[DNlogN]+q[g+lr])$, where D is the number of WPT decomposition layers (3 in [8], [20]). The key difference in the complexity of this approach and proposed time-domain approach lies in the relative complexities of their feature vectors. The proposed time-domain approach uses a 104-element feature vector; in the time-

frequency approach, the WPT coefficient feature vectors are composed of 2048 values. This leads to a very large difference in the absolute number of operations used by each approach. Table VIb quotes these figures for both the time-domain and time-frequency approaches, for the parameters in Tables III and V respectively.

TABLE VI: Operational Comparison of EMG Classification Techniques

	Operations
AR	25,584
IEMG	4,128
Kurtosis	8,208
log RMS	2,056
Skewness	6,160
RMS	4,144
Variance	6,176
MSV	4,136
Features	60,592
LDA	1,688
MLP	4,536
Total	**66,816**

(a) Time-Domain

	Operations
WPT	639,059
LDA	32,792
MLP	4,536
Total	**676,387**

(b) Time-Frequency Domain [8], [20]

As Table VIb shows, the absolute operational differences arising between the two approaches to EMG acquisition and classification are significant. The feature extraction complexity increment observed for time-frequency processing has resulted in a very substantial multi-layer WPT feature extraction process; the 60,592 operations required to extract the time-domain features is dwarfed by the 639,059 required for WPT calculation in the time-frequency approach. The smaller feature vectors which result in the time-domain approach also have the added benefit that they significantly reduce the number of operations required for LDA feature projection by almost 95% relative to the time-frequency approach.

The resulting 66,816 operations required for the entire time-domain EMG analysis process is over 90% less than the 676,387 required for the state-of-the-art time-frequency analysis. This very substantial reduction is enabled without reducing the breadth of wrist-hand movements which can be detected, or the accuracy with which they are inferred. They imply that the time-domain approach is likely to be much more suitable for deployment on embedded processors for real-time inference in a portable, battery-operated device.

V. System Implementation

To quantify the effect the significant reductions in complexity have on the ability to enable real-time inference on embedded devices, two implementations of each of the proposed time-domain approach and the state-of-the-art time-frequency approach are analysed. First, execution times are compared on a 3.6 GHz Core i7 workstation PC running MATLAB R2016a. The execution time for extracting each feature, along with the feature projection and classification steps are quoted in Table VII.

TABLE VII: MATLAB processing time Metrics

	time (ms)
AR	20.35
IEMG	0.44
Kurtosis	3.86
log RMS	0.08
Skewness	2.14
RMS	0.47
Variance	2.25
MSV	0.82
Features	30.41
LDA	0.13
MLP	29.80
Total	**60.34**

(a) Time-Domain

	time (ms)
WPT	536.84
Features	536.84
LDA	0.37
MLP	30.01
Total	**567.22**

(b) Time-Frequency Domain [8], [20]

As Table VII shows, the significantly reduced complexity of the proposed approach translates to a similar reduction in processing time relative to the time-frequency approach. Overall, execution time has reduced from 567.22 ms to 60.34 ms, a reduction of more than 89%. This is mainly due to a reduction in the processing time of the feature extraction stage from 536.4 ms to 30.4 ms.

To gauge how the reductions in complexity influence real-time EMG analysis on an embedded processor, both approaches are deployed realised on a 1.4 GHz ARM Cortex-A53 on the Raspberry Pi 3 B+ platform, and compared to the comparator time-frequency approach. The processing times of each are quoted in Table VIII.

TABLE VIII: ARM Cortex A-53 Processing Time Metrics

	time (ms)
AR	3.52
IEMG	0.07
Kurtosis	0.67
log RMS	0.02
Skewness	0.46
RMS	0.08
Variance	0.38
MSV	0.15
Features	5.35
LDA	1.80
MLP	2.60
Total	**9.75**

(a) Time-Domain

	time (ms)
WPT	196.20
Features	196.20
LDA	20.50
MLP	2.75
Total	**219.45**

(b) Time-Frequency Domain [8], [20]

Again, substantial reductions in processing time have followed the complexity reductions. As described in Table VIII, the proposed approach executes in 9.75 ms on the ARM Cortex-A53. Not only is this processing time low enough to process each 128 ms EMG window in real-time, it is over 95% lower than the equivalent metric measured from the leading

time-frequency approach, where the processing time of 219.5 ms does not support real-time processing. Given the relative difference in processing time experienced by the proposed approach and the 128 ms requirement, the frequency of the clock signal for the target processor could be substantially reduced (by a factor of over ten), without violating the real-time requirement. Given that the dynamic power consumption of synchronous digital logic reduces in proportion to the clock frequency, corresponding reductions in power consumption will follow.

Hence, to the best of the author's knowledge, the time-domain approach proposed in Section III achieves two unique contributions.

1) It is the only approach which allows analysis of EMG signals gathered from random locations on the skin's surface to support inference of as many wrist-hand movements as state-of-the-art placed-sensor systems, with comparable accuracy.
2) It is the only approach on record which can achieve this breadth and accuracy whilst enabling real-time analysis on an embedded processor suitable for integration in portable, battery operated devices. This is as a result of the complexity of the EMG analysis process being reduced by over 90% relative to the state-of-the-art in placed-sensor systems.

These benefits are significant but if the approach is to be deployed in practise it is imperative that the complexity be minimised as far as possible to maximise the operating lifetime in energy-constrained battery-operated equipment. Section VI studies techniques to achieve this optimisation.

VI. Complexity/Performance Trade-off and Optimisation

Two techniques are investigated to reduce the complexity of the time-domain EMG acquisition and classification approach:

- Reduction in the number of features
- Reduction in the number of channels

A. Feature Extraction Optimisation

Section IV illustrated how reducing the length of the feature vector relative to the time-frequency WPT technique enabled substantial reductions in complexity. One way to further optimise system cost is to reduce feature vector length still further. This has the potential to reduce classification accuracy as well as complexity and hence the objective is to minimise the feature vector length whist maintaining acceptable levels of performance.

Section III-A and Fig. 2 described how the variation of the eight selected features were dramatically different, with the variation of four (AR, IEMG, kurtosis and skewness) relatively large compared to the others. Assuming the four features with highest variation form a foundation feature-set, Fig. 5 compares the accuracy of the time-domain classification system when all k-element feature vectors $K = \{k_i\}_{i=4}^{8}$ are used. As this shows, generally as the number of features increases, so does classification accuracy. The peak classification accuracy, and the associated feature-sets are detailed in Table IX.

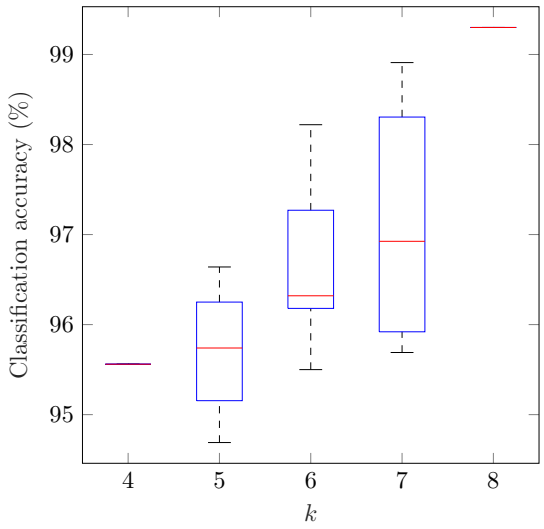

Fig. 5: Performance Variation with Feature Set Size

TABLE IX: Peak Accuracy for varying Feature Set Size

k	Feature added	Accuracy (%)
4	{AR, IEMG, kurtosis, ln RMS}	95.56
5	skewness	96.64
6	RMS-variance	98.22
7	skewness-RMS-variance	98.91
8	skewness-RMS-variance-MSV	99.30

These results are notable for a number of reasons. Even when the foundation four-element feature set is employed, the accuracy achieved - 95.6% - is highly competitive with that of previous state-of-the-art placed-sensor system. The accuracy improves steadily as further features are added to the peak of 99.3% when all the features are employed. Of particular note is the significant increase in performance between $k = 5$ and $k = 6$, which increases accuracy by almost 1.6%; in all other cases increments are less than 1%.

These results show that, even if only the base feature set is employed and the feature vector length for each channel is reduced from 13 elements to 9, classification accuracy is still highly competitive with the state-of-the-art in placed-sensor systems, but overall complexity is reduced by more than 30%.

B. Complexity measure for Channels

An alternative to employing many shorter feature vectors is to use fewer longer ones. The EMG acquisition unit used houses eight EMG sensors, but there is no reason all eight must be used. As detailed in Section IV, the complexity of each of the feature extraction, projection and classification processes are linear in the number of channels and hence if fewer channels were used, complexity would reduce in proportion.

If only a subset of the eight EMG channels are to be used, two questions must be answered - how many channels,

and which specific subset of the eight? To provide empirical evidence of the best combination, the classification accuracy of all u-element subsets of the eight EMG channels $U = \{u_i\}_{i=4}^{8}$ are employed in the time-domain EMG analysis approach. The accuracy of these subsets are summarised in Fig. 6.

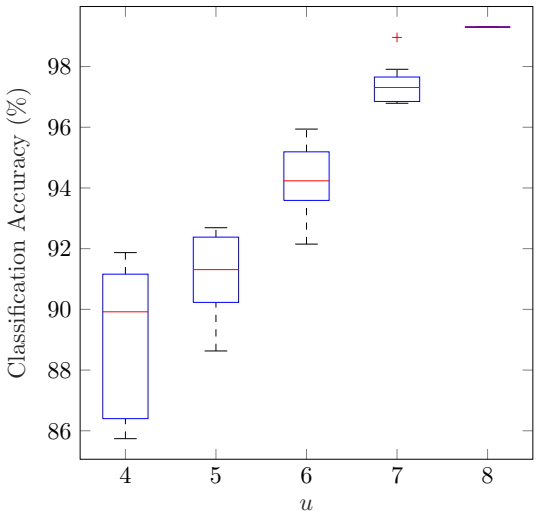

Fig. 6: Classification results for different set of channel selection.

As Fig. 6 shows, classification accuracy generally increases with the number of channels, whilst variation in the performance between specific instances of each number of channels decreases. The peak classification accuracy for each value of i is stated in Table X.

TABLE X: Peak Accuracy Variation for Channel Subsets

u	**Channels**	**Accuracy** (%)
4	$\{1, 3, 5, 7\}$	91.87
5	$\{1, 3, 4, 5, 8\}$	92.69
6	$\{3, 4, 5, 6, 7, 8\}$	98.22
7	$\{1, 2, 3, 4, 6, 7, 8\}$	98.91
8	$\{1, 2, 3, 4, 5, 6, 7, 8\}$	99.30

Table X unveils a number of further trends. When either 4 or 5 channels are used, classification accuracy is significantly lower than the state-of-the-art placed-sensor approach. However, a particularly notable increase in peak accuracy when the number of channels is increased from five (95.7%) to six (98.22%). This indicates that classification accuracy beyond that achieved by time-frequency placed-sensor systems can be maintained despite reducing the complexity of the EMG analysis process by 25%.

VII. Conclusion & Future Works

Wearables which record EMG signals from the skin's surface offer the potential for close interaction with electronic devices and virtual environments via the use of portable, battery-operated equipment. To date, though, there has been no way for such equipment to accurately detect a wide range of wrist-hand movements. Any approach which has done so assumes that the EMG signals have been gathered by sensors precisely placed over specific muscles on the forearm.

This paper has addressed this problem. Time-domain analysis of EMG signals sampled by an arm-band at a random position on the lower arm is used; it has been shown that by extracting an eight element vector of features from each of eight EMG channels, a combination of LDA-based projection MLP classification can identify nine wrist-hand movements with accuracy in excess of 99%. Not only is this accuracy in excess of that achieved by the state-of-the-art, it is achieved using significantly reduced complexity. Specifically, 66,816 operations are required for each classification, as compared to the 676,387 operations required by the state-of-the-art. This 90% complexity reduction corresponds to a similar reduction in execution time and has enabled the first recorded real-time realisation on an embedded processor suitable for integration in portable, battery-powered EMG wearables. It has further been shown how respective complexity reductions of 30% and 25% can be achieved by reducing the number of features or the number of EMG channels, all whilst maintaining state-of-the-art detection performance.

There are numerous avenues for further research. Of course, alternative time-domain features can be considered, or different combinations of feature vector length and number of channels. Another highly promising avenue, however, is to consider the use of other sensors alongside the EMG-only approach considered in this paper. The armband used, for, instance, includes an Inertial Measurement Unit (IMU), gyroscope and accelerometer; by considering the signals emanating from these, the number of EMG channels, or the number of features derived from each could be reduced still further without significant reductions in capability.

References

[1] R. Merletti and P. A. Parker, *Electromyography: Physiology, Engineering, and Non-invasive Applications*. John Wiley & Sons, 2004, vol. 11.

[2] E. Mattar, "A Survey of Bio-inspired Robotics Hands Implementation: New Directions in Dexterous Manipulation," *Robotics and Autonomous Systems*, vol. 61, no. 5, pp. 517–544, 2013.

[3] T. S. Saponas, D. S. Tan, D. Morris, and R. Balakrishnan, "Demonstrating the Feasibility of Using Forearm Electromyography for Muscle-computer Interfaces," in *Proc. SIGCHI Conference on Human Factors in Computing Systems*, ser. CHI '08. ACM, 2008, pp. 515–524.

[4] M. E. Benalcázar, C. Motoche, J. A. Zea, A. G. Jaramillo, C. E. Anchundia, P. Zambrano, M. Segura, F. B. Palacios, and M. Pérez, "Real-time Hand Gesture Recognition using the Myo Armband and Muscle Activity Detection," in *2017 IEEE Ecuador Technical Chapters Meeting (ETCM)*. IEEE, 2017, pp. 1–6.

[5] A. Boyali, N. Hashimoto, and O. Matsumoto, "Hand Posture and Gesture Recognition using MYO Armband and Spectral Collaborative Representation based Classification," in *2015 IEEE 4th Global Conf. on Consumer Electronics (GCCE)*. IEEE, 2015, pp. 200–201.

[6] T. Phienthrakul, "Armband Gesture Recognition on Electromyography Signal for Virtual Control," in *2018 10th Intl. Conf. on Knowledge and Smart Technology (KST)*. IEEE, 2018, pp. 149–153.

[7] S. Rawat, S. Vats, and P. Kumar, "Evaluating and Exploring the MYO Armband," in *Intl. Conf. on System Modeling & Advancement in Research Trends (SMART)*. IEEE, 2016, pp. 115–120.

[8] J.-U. Chu, I. Moon, and M.-S. Mun, "A Real-time EMG Pattern Recognition System Based on Linear-Nonlinear Feature Projection for a Multifunction Myoelectric Hand," *IEEE Trans. Biomedical Engineering*, vol. 53, no. 11, pp. 2232–2239, 2006.

[9] P. Yang, K. Xing, J. Huang, and Y. Wang, "A Novel Feature Reduction Method for Real-time EMG Pattern Recognition System," in *25th Chinese Control and Decision Conference (CCDC)*. IEEE, 2013, pp. 1500–1505.

[10] P. Shenoy, K. J. Miller, B. Crawford, and R. P. Rao, "Online Electromyographic Control of a Robotic Prosthesis," *IEEE Trans. Biomedical Engineering*, vol. 55, no. 3, pp. 1128–1135, 2008.

[11] S. Raurale, J. McAllister, and J. Martinez del Rincon, "EMG Acquisition and Hand Pose Classification for Bionic Hands from Randomly-Placed Sensors," in *2018 IEEE International Conference on Acoustics, Speech and Signal Processing (ICASSP)*, April 2018, pp. 1105–1109.

[12] Delsys, "Delsys EMG Sensor Placement Technical Note 101," 2016, [Online: accessed 9-July-2018].

[13] R. Merletti, A. Botter, A. Troiano, E. Merlo, and M. A. Minetto, "Technology and Instrumentation for Detection and Conditioning of the Surface Electromyographic Signal: State of the Art," *Clinical Biomechanics*, vol. 24, no. 2, pp. 122–134, 2009.

[14] M. B. I. Reaz, M. Hussain, and F. Mohd-Yasin, "Techniques of EMG Signal Analysis: Detection, Processing, Classification and Applications," *Biological Procedures Online*, vol. 8, no. 1, p. 11, 2006.

[15] M. Yoshikawa, M. Mikawa, and K. Tanaka, "Real-time Hand Motion Estimation using EMG Signals with Support Vector Machines," in *2006 SICE-ICASE Intl. Joint Conference*. IEEE, 2006, pp. 593–598.

[16] K. Englehart, B. Hudgins, P. A. Parker, and M. Stevenson, "Classification of the Myoelectric Signal using Time-Frequency-based Representations," *Medical Engineering and Physics*, vol. 21, no. 6, pp. 431–438, 1999.

[17] J. Chen, G. Wang, and G. B. Giannakis, "Nonlinear Dimensionality Reduction for Discriminative Analytics of Multiple Datasets," *IEEE Transactions on Signal Processing*, vol. 67, no. 3, pp. 740–752, Feb 2019.

[18] N. M. Kakoty and S. M. Hazarika, "Recognition of Grasp Types Through Principal Components of DWT-based EMG Features," in *2011 IEEE Intl. Conf. on Rehabilitation Robotics (ICORR)*. IEEE, 2011, pp. 1–6.

[19] A. Phinyomark, H. Hu, P. Phukpattaranont, and C. Limsakul, "Application of Linear Discriminant Analysis in Dimensionality Reduction for Hand Motion Classification," *Measurement Science Review*, vol. 12, no. 3, pp. 82–89, 2012.

[20] J.-U. Chu, I. Moon, Y.-J. Lee, S.-K. Kim, and M.-S. Mun, "A Supervised Feature-projection-based Real-time EMG Pattern Recognition for Multifunction Myoelectric Hand Control," *IEEE/ASME Trans. Mechatronics*, vol. 12, no. 3, pp. 282–290, 2007.

[21] Z. Liao and R. Couillet, "A Large Dimensional Analysis of Least Squares Support Vector Machines," *IEEE Transactions on Signal Processing*, vol. 67, no. 4, pp. 1065–1074, Feb 2019.

[22] M. A. Oskoei and H. Hu, "Application of Support Vector Machines in Upper Limb Motion Classification using Myoelectric Signals," in *2007 IEEE Intl. Conf. on Robotics and Biomimetics (ROBIO)*. IEEE, 2007, pp. 388–393.

[23] H. Xie, P. Zhou, T. Guo, B. Sivakumar, X. Zhang, and S. Dokos, "Multiscale Two-Directional Two-Dimensional Principal Component Analysis and Its Application to High-Dimensional Biomedical Signal Classification," *IEEE Trans. Biomedical Engineering*, vol. 63, no. 7, pp. 1416–1425, 2016.

[24] P. McCool, N. Chatlani, L. Petropoulakis, J. J. Soraghan, R. Menon, and H. Lakany, "Lower Arm Electromyography (EMG) Activity Detection using Local Binary Patterns," *IEEE Trans. Neural Systems and Rehabilitation Engineering*, vol. 22, no. 5, pp. 1003–1012, 2014.

[25] N. Sezgin, "A New Hand Finger Movements Classification System Based on Bicoherence Analysis of Two-channel Surface EMG Signals," *Neural Computing and Applications*, pp. 1–11, 2017.

[26] M. P. Mobarak, R. M. Guerrero, J. G. Salgado, and V. L. Dorr, "Hand Movement Classification using Transient State Analysis of Surface Multichannel EMG Ssignal," in *2014 Pan American Health Care Exchanges (PAHCE)*. IEEE, 2014, pp. 1–6.

[27] M. Sathiyanarayanan and S. Rajan, "Myo Armband for Physiotherapy Healthcare: A Case Study using Gesture Recognition Application," in *2016 8th Intl. Conf. on Communication Systems and Networks (COMSNETS)*. IEEE, 2016, pp. 1–6.

[28] A. W. Wilson, Y. G. Losier, P. A. Parker, and D. F. Lovely, "A Bus-based Smart Myoelectric Electrode/Amplifier System Requirements," *IEEE Trans. on Instrumentation and Measurement*, vol. 60, no. 10, pp. 3290–3299, 2011.

[29] K. Englehart and B. Hudgins, "A Robust, Real-time Control scheme for Multifunction Myoelectric Control," *IEEE Trans. Biomedical Engineering*, vol. 50, no. 7, pp. 848–854, 2003.

[30] A. Phinyomark, P. Phukpattaranont, and C. Limsakul, "Feature Reduction and Selection for EMG Signal Classification," *Expert Systems with Applications*, vol. 39, no. 8, pp. 7420–7431, 2012.

[31] K. Veer and T. Sharma, "A Novel Feature Extraction for Robust EMG Pattern Recognition," *Journal of Medical Engineering and technology*, vol. 40, no. 4, pp. 149–154, 2016.

[32] T. Y. Fukuda, J. O. Echeimberg, J. E. Pompeu, P. R. G. Lucareli, S. Garbelotti, R. O. Gimenes, and A. Apolinário, "Root Mean Square Value of the Electromyographic Signal in the Isometric Torque of the Quadriceps, Hamstrings and Brachial Biceps Muscles in Female Subjects," *J. Appl. Res.*, vol. 10, no. 1, pp. 32–39, 2010.

[33] M. S. Stein and J. A. Nossek, "A Pessimistic Approximation for the Fisher Information Measure," *IEEE Transactions on Signal Processing*, vol. 65, no. 2, pp. 386–396, Jan 2017.

[34] H. Mathis, "On the Kurtosis of Digitally Modulated Signals with Timing Offsets," in *2001 IEEE Third Workshop on Signal Processing Advances in Wireless Communications (SPAWC)*. IEEE, 2001, pp. 86–89.

[35] H. Kirshner, M. Unser, and J. P. Ward, "On the Unique Identification of Continuous-Time Autoregressive Models From Sampled Data," *IEEE Transactions on Signal Processing*, vol. 62, no. 6, pp. 1361–1376, March 2014.

[36] H. Kato, M. Taniguchi, and M. Honda, "Statistical Analysis for Multiplicatively Modulated Nonlinear Autoregressive Model and its Applications to Electrophysiological Signal Analysis in Humans," *IEEE Transactions on Signal Processing*, vol. 54, no. 9, pp. 3414–3425, Sep. 2006.

[37] D. Tkach, H. Huang, and T. A. Kuiken, "Study of Stability of Time-domain Features for Electromyographic Pattern Recognition," *Journal of Neuroengineering and Rehabilitation*, vol. 7, no. 1, p. 21, 2010.

[38] H. Akaike, "A New Look at the Statistical Model Identification," *IEEE Trans. on Automatic Control*, vol. 19, no. 6, pp. 716–723, 1974.

[39] G. Kitagawa and W. Gersch, "A Smoothness Priors Time-Varying AR Coefficient Modeling of Nonstationary Covariance Time Series," *IEEE Trans. on Automatic Control*, vol. 30, no. 1, pp. 48–56, 1985.

[40] A. Tharwat, T. Gaber, A. Ibrahim, and A. E. Hassanien, "Linear Discriminant Analysis: A Detailed Tutorial," *AI Communications*, vol. 30, pp. 169–190,, 05 2017.

[41] S. Haykin, *Neural Networks: A Comprehensive Foundation*, 2nd ed. Upper Saddle River, NJ, USA: Prentice Hall PTR, 1998.

[42] Y. Ji, S. Sun, and H.-B. Xie, "Stationary Wavelet-based Two-directional Two-dimensional Principal Component Analysis for EMG Signal Classification," *Measurement Science Review*, vol. 17, no. 3, pp. 117–124, 2017.

[43] T. H. Cormen, C. E. Leiserson, R. L. Rivest, and C. Stein, *Introduction to Algorithms, Third Edition*, 3rd ed. The MIT Press, 2009.